

Article

Preparation and Photocatalytic Properties of $\text{Sr}_{2-x}\text{Ba}_x\text{Ta}_3\text{O}_{10-y}\text{N}_z$ Nanosheets

Shintaro Ida^{1,2,3,*}, Yohei Okamoto¹, Hideshisa Hagiwara^{1,2} and Tatsumi Ishihara^{1,2}

¹ Department of Applied Chemistry, Faculty of Engineering, Kyushu University, Motoooka 744, Nishi-ku, Fukuoka 819-0395, Japan; E-Mails: okamonian@gmail.com (Y.O.); h.hagiwara@cstf.kyushu-u.ac.jp (H.H.); ishihara@cstf.kyushu-u.ac.jp (T.I.)

² International Institute for Carbon Neutral Energy Research (I2CNER), Kyushu University, Motoooka 744, Nishi-ku, Fukuoka 819-0395, Japan

³ Precursory Research for Embryonic Science and Technology (PRESTO), Japan Science and Technology Agency, 4-1-8 Honcho Kawaguchi, Saitama 332-0012, Japan

* Author to whom correspondence should be addressed; E-Mail: s-ida@cstf.kyushu-u.ac.jp; Tel.: +81-92-802-2869; Fax: +81-92-802-2871.

Received: 11 November 2012; in revised form: 17 December 2012 / Accepted: 9 January 2013 / Published: 2013

Abstract: $\text{Sr}_{2-x}\text{Ba}_x\text{Ta}_3\text{O}_{10-y}\text{N}_z$ ($x = 0.0, 0.5, 1.0$) nanosheets were prepared by exfoliating layered perovskite compounds ($\text{CsSr}_{2-x}\text{Ba}_x\text{Ta}_3\text{O}_{10-y}\text{N}_z$). The $\text{Sr}_{1.5}\text{Ba}_{0.5}\text{Ta}_3\text{O}_{9.7}\text{N}_{0.2}$ nanosheet showed the highest photocatalytic activity for H_2 production from the water/methanol system among the $\text{Sr}_{2-x}\text{Ba}_x\text{Ta}_3\text{O}_{9.7}\text{N}_{0.2}$ nanosheets prepared. In addition, Rh-loaded $\text{Sr}_{1.5}\text{Ba}_{0.5}\text{Ta}_3\text{O}_{9.6}\text{N}_{0.3}$ nanosheet showed the photocatalytic activity for oxygen and hydrogen production from water. The ratio of hydrogen to oxygen evolved was around two. These results indicate that the Rh-loaded $\text{Sr}_{1.5}\text{Ba}_{0.5}\text{Ta}_3\text{O}_{9.6}\text{N}_{0.3}$ nanosheet is a potential catalyst for photocatalytic water splitting.

Keywords: nanosheet; water splitting; exfoliation

1. Introduction

Nanosheets prepared by exfoliation of layered materials are single crystals with a thicknesses on the order of molecular sizes [1–9]. For example, oxide [1–5], hydroxide [6–8] and grapheme nanosheets [9] have been investigated for various potential applications, including fillers, cosmetics, ultraviolet

protection films and high-speed transistors. We have been focusing on the photocatalytic property of nanosheets. Hydrogen production from water using semiconducting photocatalysts has attracted attention as a clean solar hydrogen-generation system [10,11]. A high crystallinity and a large surface area are critical for realizing high-efficiency photocatalysts; nanosheets satisfy both these requirements. In addition, the molecular size thickness of nanosheets also improves their quantum efficiency. For conventional powder catalysts with particle diameters in the range 0.5–3.0 μm , photoexcited electrons and holes generated within them have to travel a long distance to the surface to react with water. However, electrons and holes may recombine or become trapped at defect sites during this long trip to the surface, which can reduce their hydrogen production efficiency. On the other hand, photoexcited electrons and holes generated in a nanosheet can reach its surface without encountering obstructions due to its ultrathin thickness and high crystallinity. For example, $[\text{Nb}_6\text{O}_{17}]^{4-}$ and $[\text{Ca}_2\text{Nb}_3\text{O}_{10}]^-$ nanosheets have been reported to have higher catalytic efficiencies than their parent compounds [12–16]. Unfortunately, these nanosheets have large band gaps and are thus not active under visible light irradiation.

Recently, $\text{Ca}_2\text{Ta}_3\text{O}_{9.7}\text{N}_{0.2}$ nanosheet was prepared from $\text{CsCa}_2\text{Ta}_3\text{O}_{9.7}\text{N}_{0.2}$ [17]. The $\text{Ca}_2\text{Ta}_3\text{O}_{9.7}\text{N}_{0.2}$ nanosheet showed a photocatalytic activity under visible light irradiation. However, there have been only a few reports on the photocatalytic property of nitrogen-doped or oxynitride nanosheets [18,19]. In this study, we investigated the effect of A site ions in $\text{Sr}_{2-x}\text{Ba}_x\text{Ta}_3\text{O}_{10-y}\text{N}_z$ nanosheets on photocatalytic activity.

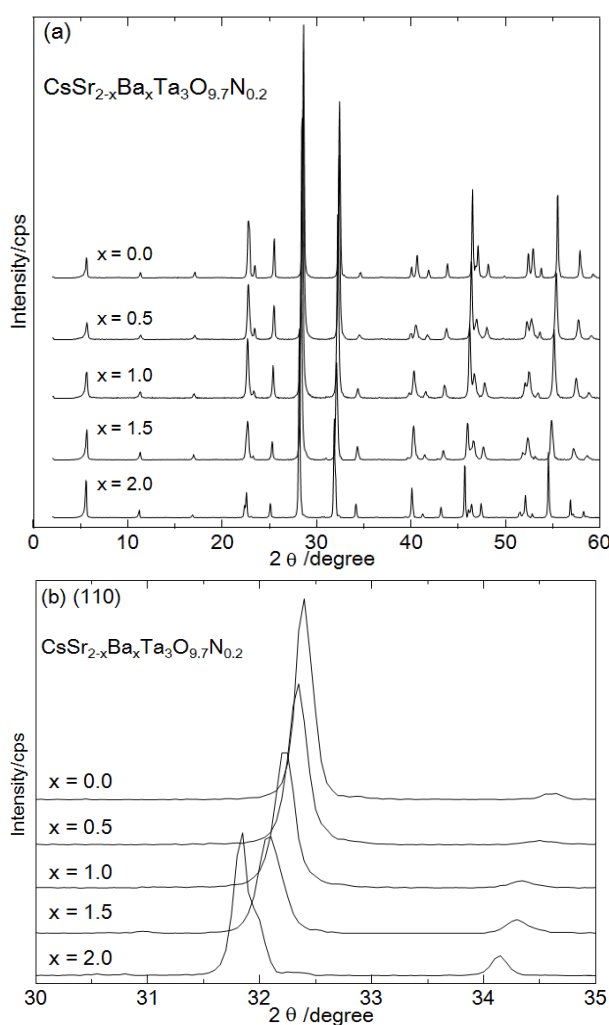
2. Results and Discussion

$\text{CsAE}_2\text{Ta}_3\text{O}_{10}$ (AE = Ca, Sr, Ba) layered oxides have the $n = 3$ structure of the Dion-Jacobson series of phases. Figure 1a shows XRD patterns of $\text{CsSr}_{2-x}\text{Ba}_x\text{Ta}_3\text{O}_{10-y}\text{N}_z$ ($x = 0.0, 0.5, 1.0, 1.5, 2.0$). The N/O molar ratio of $\text{CsSr}_{2-x}\text{Ba}_x\text{Ta}_3\text{O}_{10-y}\text{N}_z$ prepared at 800 $^\circ\text{C}$ was determined by the HNO analyzer to be approximately 2% ($\text{CsSr}_{2-x}\text{Ba}_x\text{Ta}_3\text{O}_{9.7}\text{N}_{0.2}$). Sr^{2+} and Ba^{2+} ions occupy A sites in the host perovskite layer and Ta^{5+} ions occupy the B sites. The XRD patterns of the $\text{CsSr}_{2-x}\text{Ba}_x\text{Ta}_3\text{O}_{9.7}\text{N}_{0.2}$ corresponded to that of $\text{CsSr}_2\text{Ta}_3\text{O}_{10}$ powder, which has tetragonal symmetry with the P4/mmm space group [20]. There were no other significant differences in the diffraction patterns of the layered compounds before and after calcination in NH_3 at 800 $^\circ\text{C}$, which agrees with the result reported previously [21]. This indicates that nitrogen partially substituted oxygen in the layered oxide without altering the crystal phase. The peaks ascribed to the (110) were shifted to smaller angles with an increasing amount of Ba, as shown in Figure 1b. These peak shifts indicate the successful preparation of $\text{CsSr}_{2-x}\text{Ba}_x\text{Ta}_3\text{O}_{9.7}\text{N}_{0.2}$, because the ionic radius of Ba^{2+} (0.161 nm) is slightly larger than that of Sr^{2+} (0.144 nm).

Nanosheets were prepared by exfoliating the layered perovskite compounds ($\text{CsSr}_{2-x}\text{Ba}_x\text{Ta}_3\text{O}_{9.7}\text{N}_{0.2}$) via proton exchange and two-step intercalation of ethylamine and tetrabutylammonium ions. The Cs ions in the layered compounds were exchanged with protons by acid exchange. The protonated forms were stirred in ethylamine (EA) aqueous solution to intercalate the EA into the interlayer. The EA-intercalated layered compounds were stirred in tetrabutylammonium hydroxide (TBAOH) aqueous solution to exfoliate into nanosheets. The nanosheets could not be fabricated directly from the protonated forms, since TBA^+ ions are not intercalated into the protonated forms without the EA intercalation step. This strongly suggests that EA intercalation is an essential step in nanosheet

synthesis. The process of intercalation of amine into the protonated form is commonly understood as an acid base reaction between interlayer protons (Brønsted acid) and amines (Brønsted base). This process generally depends on the size and charge density of the guest species and the hydration state of the layered compounds. A TBA⁺ ion is a quaternary ammonium ion with four butyl groups attached to a positively charged nitrogen atom at the center. The diameter of a TBA⁺ ion is 0.8 nm, which is larger than the interlayer distance of H-Sr_{2-x}Ba_xTa₃O_{9.7}N_{0.2} (around 0.2 nm). This relatively large diameter of TBA⁺ ion may have been one of the possible reasons for the current finding.

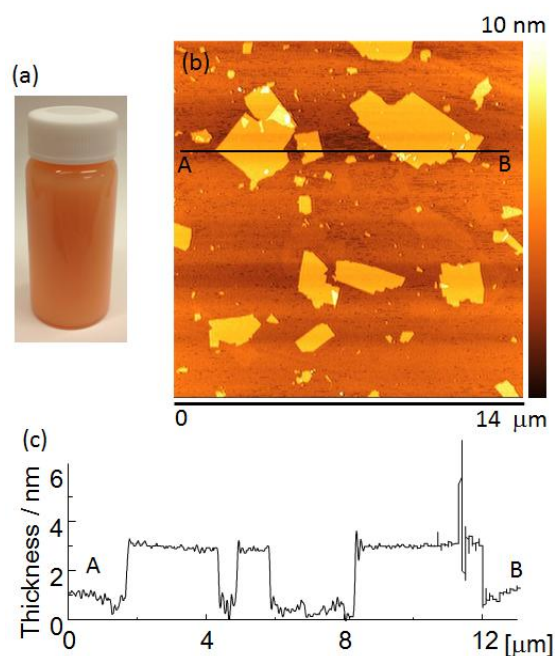
Figure 1. X-ray diffraction (XRD) patterns of CsSr_{2-x}Ba_xTa₃O_{9.7}N_{0.2} ($x = 0.0, 0.5, 1.0, 1.5, 2.0$), (a) wide scan (2–60 degree) and (b) narrow scan (30–35 degree).



Exfoliation of layered compounds to nanosheets was confirmed by AFM observations. The layered compounds ($x = 0, 0.5, 1.0$) were exfoliated to nanosheets, whereas the layered compounds ($x = 1.5, 2.0$) could not be exfoliated. Organic amines, which were used as exfoliation reagents, were not intercalated into the protonated layered compounds ($x = 1.5, 2.0$). The ratio of nitrogen to oxygen in the nanosheet powder was around 2% (Sr_{2-x}Ba_xTa₃O_{9.7}N_{0.2}; $x = 0.0, 0.5, 1.0$), which was almost the same as that of the parent layered material (2%). Figure 2a shows the appearance of a Sr_{1.5}Ba_{0.5}Ta₃O_{10-y}N_z suspension. The suspension was orange in color due to nitrogen doping. Figure 2b shows an AFM image of Sr₂Ta₃O_{10-y}N_z nanosheets. They had lateral dimensions of about 0.3–5.0 μm. Figure 2c shows

a cross-sectional profile of a nanosheet measured between points A and B in Figure 2b. The nanosheets were approximately 2.8–3.1 nm thick, which is approximately 1.3 nm thicker than the theoretical perovskite blocks of the parent compound, estimated from crystallographic data. The difference between the nanosheet thickness estimated from AFM observations, and the theoretically calculated thickness is due to the absorption of water and amine [22]. However, the nanosheet suspension contained bilayer and trilayer nanosheets in addition to monolayer nanosheets.

Figure 2. (a) The appearance of a nanosheet suspension, (b) atomic force microscopy (AFM) image and (c) cross-sectional profile of mono-layer nanosheet.



Photocatalytic activities of $\text{Sr}_{2-x}\text{Ba}_x\text{Ta}_3\text{O}_{9.7}\text{N}_{0.2}$ ($x = 0.0, 0.5, 1.0$) nanosheets were tested in a water/ethanol system. Methanol was employed as the sacrificial reagent. All samples showed the photocatalytic activity under visible light irradiation as shown in Table 1. The H_2 production rate under visible light irradiation of $\text{Sr}_{1.5}\text{Ba}_{0.5}\text{Ta}_3\text{O}_{9.7}\text{N}_{0.2}$ ($x = 0.5$) nanosheet was the highest ($1.44 \mu\text{M/h}$) among the $\text{Sr}_{2-x}\text{Ba}_x\text{Ta}_3\text{O}_{9.7}\text{N}_{0.2}$ ($x = 0.0, 0.5, 1.0$) nanosheets prepared. Next, the calcination temperature for nitridation was optimized. Figure 3 shows XRD patterns of $\text{CsSr}_{1.5}\text{Ba}_{0.5}\text{Ta}_3\text{O}_{10-y}\text{N}_z$ prepared at 750–900 °C. All XRD patterns of the layered compounds prepared at 750–850 °C corresponded to that of $\text{CsSr}_2\text{Ta}_3\text{O}_{10}$ powder, whereas the layered compound prepared at 900 °C had an impurity phase (Ta_3N_5). Therefore, the photocatalytic activity of the nanosheets prepared at 750–850 °C was investigated.

Table 1. Photocatalytic activities of $\text{Sr}_{2-x}\text{Ba}_x\text{Ta}_3\text{O}_{9.7}\text{N}_{0.2}$ ($x = 0.0, 0.5, 1.0$) nanosheets for H_2 production from water/ethanol system under irradiation.

A site element	Full arc irradiation ($\mu\text{mol/h}$)	Visible light irradiation ($\mu\text{mol/h}$)
Sr_2	302.2	0.27
$\text{Sr}_{1.5}\text{Ba}_{0.5}$	260.6	1.44
SrBa	239.6	1.12

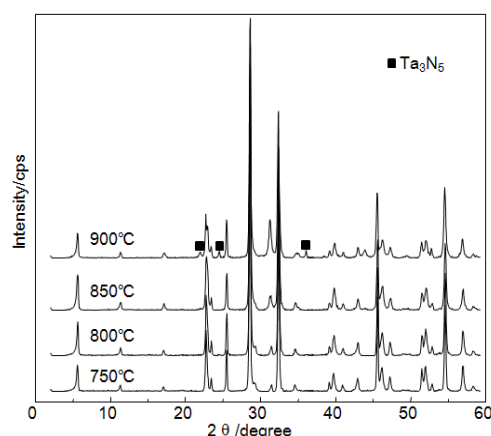
Figure 3. XRD patterns of $\text{CsSr}_{1.5}\text{Ba}_{0.5}\text{Ta}_3\text{O}_{10-y}\text{N}_z$ prepared at 750–900 °C.

Figure 4 shows the photocatalytic activities for H_2 production in a methanol aqueous solution under visible light irradiation of $\text{Sr}_{1.5}\text{Ba}_{0.5}\text{Ta}_3\text{O}_{10-y}\text{N}_z$ nanosheets. Rh (0.15 wt.%) was loaded on the nanosheet as a co-catalyst. The amounts of H_2 evolved increased approximately linearly with increasing the irradiation time. The $\text{Sr}_{1.5}\text{Ba}_{0.5}\text{Ta}_3\text{O}_{10-y}\text{N}_z$ nanosheets prepared from layered compound calcinated at 850 °C showed the highest activity for photocatalytic H_2 production. The H_2 production rate was 2.18 $\mu\text{M}/\text{h}$.

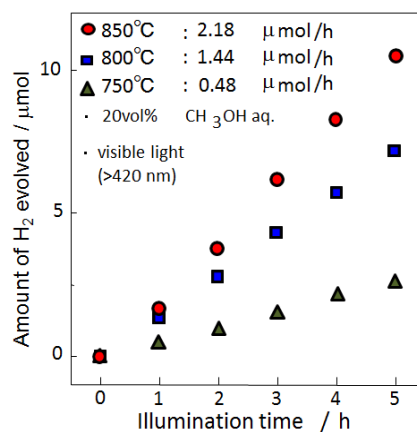
Figure 4. Photocatalytic activities for H_2 production from a system in aqueous 20 vol.% methanol solutions under visible light (>420 nm) irradiation of Rh (0.15 wt.%) loaded $\text{CsSr}_{1.5}\text{Ba}_{0.5}\text{Ta}_3\text{O}_{10-y}\text{N}_z$ nanosheet exfoliated from layered compounds prepared at 750–850 °C. The amount of catalyst: 200 mg, catalyst: 0.15 wt.% Rh-loaded samples.

Figure 5 shows diffuse reflectance UV-vis spectra of $\text{CsSr}_{1.5}\text{Ba}_{0.5}\text{Ta}_3\text{O}_{10-y}\text{N}_z$ prepared at 750–850 °C. They contain two absorption bands: one around 500–600 nm and the other around 300–500 nm. The first absorption is due to excitation from the N 2p orbital to the Ta 5d orbital, while the second absorption band corresponds to excitation from the O 2p orbital to the Ta 5d orbital. $\text{CsSr}_{1.5}\text{Ba}_{0.5}\text{Ta}_3\text{O}_{10-y}\text{N}_z$ prepared at 850 °C had the strongest absorption band in the visible light region in three samples. The ratio of nitrogen to oxygen in the nanosheet powder was around 3%. The chemical composition was $\text{Sr}_{1.5}\text{Ba}_{0.5}\text{Ta}_3\text{O}_{9.6}\text{N}_{0.3}$. The ratio of nitrogen to oxygen in the nanosheet

prepared from the layered compound calcinated at 850 °C was higher than that calcinated at 800 °C. The ratio of nitrogen to oxygen might be related to the photocatalytic activity under visible light irradiation.

Figure 5. Diffuse reflectance ultra-violet (UV)-vis absorption spectra of $\text{CsSr}_{1.5}\text{Ba}_{0.5}\text{Ta}_3\text{O}_{10-y}\text{N}_z$ prepared at 750–900 °C.

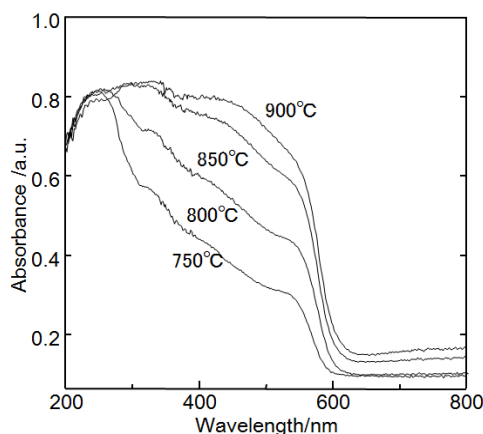
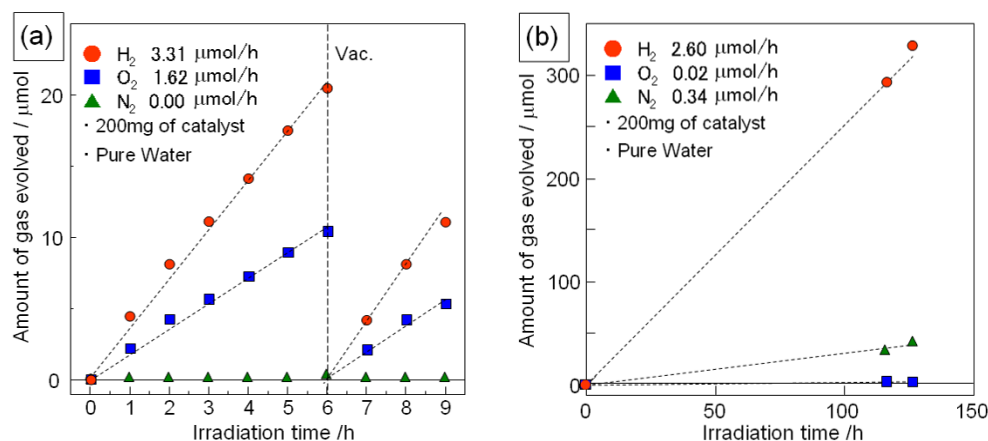


Figure 6 shows the photocatalytic activity for water splitting over $\text{Sr}_{1.5}\text{Ba}_{0.5}\text{Ta}_3\text{O}_{9.6}\text{N}_{0.3}$ (nanosheet) and $\text{H-Sr}_{1.5}\text{Ba}_{0.5}\text{Ta}_3\text{O}_{9.6}\text{N}_{0.3}$ (protonated layered compound). The chemical composition of the nanosheet sample was almost the same as that of the protonated layered compound. As the co-catalyst, Rh (0.15 wt.%) was loaded on the catalyst. In the case of the nanosheet sample, both oxygen and hydrogen were generated and the slopes for the amounts of hydrogen and oxygen evolved from the reaction remained constant during the reaction. The ratio of hydrogen to oxygen evolved was around 2:1. These results indicate that the Rh-loaded $\text{Sr}_{1.5}\text{Ba}_{0.5}\text{Ta}_3\text{O}_{9.6}\text{N}_{0.3}$ nanosheet is a potential catalyst for the photocatalytic splitting of water into hydrogen and oxygen. In the case of Rh-loaded $\text{H-Sr}_{1.5}\text{Ba}_{0.5}\text{Ta}_3\text{O}_{9.6}\text{N}_{0.3}$ (protonated layered compound), hydrogen was generated from pure water, however there was no oxygen generated from this system. In contrast, nitrogen was detected from this system. This nitrogen might be due to decomposition of the $\text{H-Sr}_{1.5}\text{Ba}_{0.5}\text{Ta}_3\text{O}_{9.6}\text{N}_{0.3}$ during the photocatalytic reaction, which is currently being investigated.

Figure 6. Time course of photocatalytic hydrogen and oxygen generation from pure water under irradiation (full arc of 500 W Xe lamp); (a) Rh (0.15wt.%) loaded $\text{Ca}_{1.5}\text{Ba}_{0.5}\text{Ta}_3\text{O}_{9.6}\text{N}_{0.3}$ nanosheets and (b) Rh (0.15 wt.%) loaded $\text{H-Ca}_{1.5}\text{Ba}_{0.5}\text{Ta}_3\text{O}_{9.6}\text{N}_{0.3}$.



3. Experimental Section

The parent layered oxides ($\text{CsSr}_{2-x}\text{Ba}_x\text{Ta}_3\text{O}_{10}$) were prepared from CsCO_3 (95.0% Wako), $\text{Sr}(\text{OOCCH}_3)_2 \cdot \text{H}_2\text{O}$ (99.0% Wako), $\text{Ba}(\text{OOCCH}_3)_2 \cdot \text{H}_2\text{O}$ (99.0% Wako) and Ta_2O_5 (99.9% Wako), according to the literature [20]. The mixture of these reagents was calcinated at 1000 °C for 10 h. An excess of alkali metal carbonate (50 mol.%) was added to compensate for the loss due to volatilization of the alkali component. The parent layered oxide prepared was converted into the layered oxynitride, $\text{CsSr}_{2-x}\text{Ba}_x\text{O}_{10-y}\text{N}_z$ by calcination at 800 °C under NH_3 flow (100 mL/min) for 6 h. The Cs ions in the layered compounds were exchanged with protons by acid exchange with 3 M HCl solution for a week. After proton exchange, the powder was washed in several changes of water by centrifugation. The protonated form (1.0 g) was stirred in 100 mL of a 1.0 M ethylamine (EA) aqueous solution to intercalate the EA into the interlayer for 5 days. The EA-intercalated layered compounds (1.0 g) was stirred for one week in 150 mL of a 0.025 M tetrabutylammonium hydroxide (TBAOH) aqueous solution to exfoliate into nanosheets. The separation of unexfoliated powder was performed by spontaneous precipitation for 1 day, and the supernatant was used as a nanosheet suspension. The nanosheet concentration was calculated from the powder obtained by drying the nanosheet suspension at 500 °C. The nanosheet suspension had a concentration of about 2.0 g/L.

A photocatalytic reaction was performed using a conventional closed circulation system. A quartz reaction cell was irradiated by light from an external light source. During the reaction, the suspension was mixed using a magnetic stirring bar. Ar gas (initial pressure: 18.3 kPa) was used as the circulating carrier gas. The amounts of H_2 and O_2 formed were measured by gas chromatography, which was connected to a conventional volumetric circulating line by a vacuum pump. 200 mL of water or 20 vol.% methanol aqueous solution was used as the reaction solution. The amounts of catalyst were 200 or 10 mg. Co-catalysts were photodeposited on nanosheets in 20 vol.% methanol aqueous solution (100 mL of nanosheet suspension, 40 mL of methanol, 30 mL of water) containing $\text{RhCl}_3 \cdot 3\text{H}_2\text{O}$ (99.5%, Wako) by irradiation with the 500 W Xe lamp for 12 h. The loading amount was adjusted by changing the amount of $\text{RhCl}_3 \cdot 3\text{H}_2\text{O}$. After loading the co-catalyst, a cellophane tube filled with 0.01 M H_2SO_4 aqueous solution was immersed in the nanosheet suspension while stirring constantly. This resulted in nanosheet deposition due to proton absorption. The deposited nanosheets were washed in several changes of water by centrifugation to remove residual TBAOH. The nanosheet paste obtained by centrifugation was used without drying for photocatalytic activity evaluations. In the case of the photocatalytic hydrogen evolution test from methanol aqueous solution, the photocatalytic activity was evaluated using the nanosheet suspension used for loading the co-catalyst without any change.

The crystal structure was analyzed by X-ray powder diffraction (Cu $\text{K}\alpha$ radiation; RINT-2500, Rigaku, Tokyo, Japan). The oxygen-to-nitrogen ratio was determined by a HNO analyzer (EMGA-930, Horiba, Kyoto, Japan). UV-vis absorption spectra were obtained by a reflection method using a spectrophotometer (U-3310, HITACHI, Tokyo, Japan) with an integrating sphere. The thickness of the exfoliated nanosheets was measured by atomic force microscopy (AFM) (Nano-cute, Seiko Instruments Inc., Chiba, Japan). The H_2 , O_2 and N_2 gases generated in the photocatalytic reaction were measured by a gas chromatography with a thermal conductivity detector (GC-8A, Shimadzu Corp.,

Kyoto, Japan). 500 W Xe-lamp (SX-UI500XQ, USHIO, Tokyo, Japan) was used as a light source for the photocatalytic reaction.

4. Conclusions

$\text{Sr}_{2-x}\text{Ba}_x\text{Ta}_3\text{O}_{10-y}\text{N}_z$ ($x = 0.0, 0.5, 1.0$) nanosheets were prepared by exfoliating layered perovskite compounds ($\text{CsSr}_{2-x}\text{Ba}_x\text{Ta}_3\text{O}_{10-y}\text{N}_z$) via proton exchange and two-step intercalation of ethylamine and tetrabutylammonium ions. The nanosheets were approximately 2.8–3.1 nm thick, which is approximately 1.3 nm thicker than the theoretical perovskite blocks of the parent compound due to water and amine absorption. The $\text{Sr}_{1.5}\text{Ba}_{0.5}\text{Ta}_3\text{O}_{9.7}\text{N}_{0.2}$ nanosheet showed the highest photocatalytic activity for H_2 production from the water/methanol system among the $\text{Sr}_{2-x}\text{Ba}_x\text{Ta}_3\text{O}_{9.7}\text{N}_{0.2}$ nanosheets prepared. In addition, Rh-loaded $\text{Sr}_{1.5}\text{Ba}_{0.5}\text{Ta}_3\text{O}_{9.6}\text{N}_{0.3}$ nanosheet showed the photocatalytic activity for oxygen and hydrogen production from water. The ratio of hydrogen to oxygen evolved was around two. These results indicate that the Rh-loaded $\text{Sr}_{1.5}\text{Ba}_{0.5}\text{Ta}_3\text{O}_{9.6}\text{N}_{0.3}$ nanosheet is a potential catalyst for photocatalytic splitting. In contrast, the protonated layered compound, $\text{H-Sr}_{1.5}\text{Ba}_{0.5}\text{Ta}_3\text{O}_{9.6}\text{N}_{0.3}$, exhibited no photocatalytic activity for O_2 production from water, while nitrogen was detected from this system. This nitrogen might be due to decomposition of the $\text{H-Sr}_{1.5}\text{Ba}_{0.5}\text{Ta}_3\text{O}_{9.6}\text{N}_{0.3}$ during the photocatalytic reaction, which is currently being investigated.

Acknowledgments

This work was supported by JST PRESTO program.

Conflict of Interest

There is no conflict of interest.

References

1. Sasaki, T.; Watanabe, M.; Hashizume, H.; Yamada, H.; Nakazawa, H. Macromolecule-like aspects for a colloidal suspension of an exfoliated titanate. Pairwise association of nanosheets and dynamic reassembling process initiated from it. *J. Am. Chem. Soc.* **1996**, *118*, 8329–8335.
2. Schaak, R.E.; Mallouk, T.E. Self-assembly of tiled perovskite monolayer and multilayer thin films. *Chem. Mater.* **2000**, *12*, 2513–2516.
3. Han, Y.-S.; Park, I.; Choy, J.-H. Exfoliation of layered perovskite, $\text{KCa}_2\text{Nb}_3\text{O}_{10}$, into colloidal nanosheets by a novel chemical process. *J. Mater. Chem.* **2001**, *11*, 1277–1282.
4. Abe, R.; Shinohara, K.; Tanaka, A.; Hara, M.; Kondo, J.N.; Domen, K. Preparation of porous niobium oxide by the exfoliation of $\text{K}_4\text{Nb}_6\text{O}_{17}$ and its photocatalytic activity. *J. Mater. Res.* **1998**, *13*, 861–865.
5. Ida, S.; Ogata, C.; Unal, U.; Izawa, K.; Inoue, T.; Altuntasoglu, O.; Matsumoto, Y. Preparation of a blue luminescent nanosheet derived from layered perovskite $\text{Bi}_2\text{SrTa}_2\text{O}_9$. *J. Am. Chem. Soc.* **2007**, *129*, 8956–8957.
6. Nadeau, P.H.; Wilson, M.J.; McHardy, W.J.; Tait, J.M. Interstratified clays as fundamental particles. *Science* **1984**, *225*, 923–925.

7. Ma, R.; Liu, Z.; Takada, K.; Iyi, N.; Bando, Y.; Sasaki, T. Synthesis and exfoliation of Co^{2+} - Fe^{3+} layered double hydroxides: An innovative topochemical approach. *J. Am. Chem. Soc.* **2007**, *129*, 5257–5263.
8. Ida, S.; Shiga, D.; Koinuma, M.; Matsumoto, Y. Synthesis of hexagonal nickel hydroxide nanosheets by exfoliation of layered nickel hydroxide intercalated with dodecyl sulfate ions. *J. Am. Chem. Soc.* **2008**, *130*, 14038–14039.
9. Novoselov, K.S.; Geim, A.K.; Morozov, S.V.; Jiang, D.; Zhang, Y.; Dubonos, S.V.; Grigorieva, I.V.; Firsov, A.A. Electric field effect in atomically thin carbon films. *Science* **2004**, *306*, 666–669.
10. Kato, H.; Asakura, K.; Kudo, A. Highly efficient water splitting into H_2 and O_2 over lanthanum-doped NaTaO_3 photocatalysts with high crystallinity and surface nanostructure. *J. Am. Chem. Soc.* **2003**, *125*, 3082–3089.
11. Maeda, K.; Teramura, K.; Lu, D.; Takata, T.; Saito, N.; Inoue, Y.; Domen, K. Photocatalyst releasing hydrogen from water. *Nature* **2006**, *440*, 295.
12. Abe, R.; Shinohara, K.; Tanaka, A.; Hara, M.; Kondo, J.N.; Domen, K. Preparation of porous niobium oxides by soft-chemical process and their photocatalytic activity. *Chem. Mater.* **1997**, *9*, 2179–2184.
13. Ebina, Y.; Sasaki, T.; Harada, M.; Watanabe, M. Restacked perovskite nanosheets and their Pt-loaded materials as photocatalysts. *Chem. Mater.* **2002**, *14*, 4390–4395.
14. Hata, H.; Kobayashi, Y.; Bojan, V.; Youngblood, W.J.; Mallouk, T.E. Direct deposition of trivalent rhodium hydroxide nanoparticles onto a semiconducting layered calcium niobate for photocatalytic hydrogen evolution. *Nano Lett.* **2008**, *8*, 794–799.
15. Comptons, O.C.; Mullet, C.H.; Chiang, S.; Osterloh, F.E. A Building block approach to photochemical water-splitting catalysts based on layered niobate nanosheets. *J. Phys. Chem. C* **2008**, *112*, 6202–6208.
16. Okamoto, Y.; Ida, S.; Hyodo, J.; Hagiwara, H.; Ishihara, T. Synthesis and photocatalytic activity of rhodium-doped calcium niobate nanosheets for hydrogen production from a water/methanol system without cocatalyst loading. *J. Am. Chem. Soc.* **2011**, *133*, 18034–18037.
17. Ida, S.; Okamoto, Y.; Matsuka, M.; Hagiwara, H.; Ishihara, T. Preparation of tantalum-based oxynitride nanosheets by exfoliation of a layered oxynitride, $\text{CsCa}_2\text{Ta}_3\text{O}_{10-x}\text{N}_y$ and their photocatalytic activity. *J. Am. Chem. Soc.* **2012**, *134*, 15773–15782.
18. Liu, G.; Wang, L.; Sun, C.; Chen, Z.; Yan, X.; Cheng, L.; Cheng, H.-M.; Lu, G.Q. Nitrogen-doped titania nanosheets towards visible light response. *Chem. Commun.* **2009**, doi:10.1039/B820483G.
19. Matsumoto, Y.; Koinuma, M.; Iwanaga, Y.; Sato, T.; Ida, S. N doping of oxide nanosheets. *J. Am. Chem. Soc.* **2009**, *131*, 6644–6645.
20. Toda, K.; Teranishi, T.; Ye, Z.-G.; Sato, M.; Hinatsu, Y. Structural chemistry of new ion-exchangeable tantalates with layered perovskite structure: New Dion-Jacobson phase $\text{M}\text{Ca}_2\text{Ta}_3\text{O}_{10}$ (M = alkali metal) and Ruddlesden-Popper phase $\text{Na}_2\text{Ca}_2\text{Ta}_3\text{O}_{10}$. *Mater. Res. Bull.* **1999**, *34*, 971–982.

21. Zong, X.; Sun, C.; Chen, Z.; Mukherji, A.; Wu, H.; Zou, J.; Smith, S.C.; Lu, G.Q.; Wang, L. Nitrogen doping in ion-exchangeable layered tantalate towards visible-light induced water oxidation. *Chem. Commun.* **2011**, *47*, 6293–6295.
22. Izawa, K.; Yamada, T.; Unal, U.; Ida, S.; Altuntasoglu, O.; Koinuma, M.; Matsumoto, Y. Photoelectrochemical oxidation of methanol on oxide nanosheets. *J. Phys. Chem. B* **2006**, *110*, 4645–4650.

© 2013 by the authors; licensee MDPI, Basel, Switzerland. This article is an open access article distributed under the terms and conditions of the Creative Commons Attribution license (<http://creativecommons.org/licenses/by/3.0/>).